Predictions of New Semiconductor of Transition Metal Structures and Their Properties

1993 Jpn. J. Appl. Phys. 32 14

(http://iopscience.iop.org/1347-4065/32/S3/14)

Proc. 9th Int. Conf. Ternary and Multinary Compounds, Yokohama, 1993
Jpn. J. Appl. Phys. Vol. 32 (1993) Suppl. 32-3, pp. 14-21

Invited

Predictions of New Semiconductor of Transition Metal Structures and Their Properties

Alex ZUNGER

National Renewable Energy Laboratory, Golden, Colorado 80401, USA

(Received September 11, 1993)

I describe how one can use the "Cluster Expansion Method" to predict systematically what are the thermodynamically stable crystal structures on a given lattice type. The method is used to illustrate how hitherto unsuspected ordered compounds can be identified, including new transition metal intermetallics and ternary semiconductors.

KEYWORDS: ternary semiconductors, chalcopyrites, phase-diagram, theory, new materials, transition metal compounds, stannite, cluster expansion

1. Introduction

Perhaps the most intriguing aspect of the spectacular success that semiconductor-based "high technology" has had in the past 50 years is the tiny number of core materials on which these technologies are based. Even considering a broad range of semiconductor devices—transistors, computer chips, solid state lasers, detectors, solar cells, light-emitting diodes, etc.—one finds but ~O(10) basic semiconductors that enable these technologies. This is a strikingly narrow material base, considering the number of core materials that enable other technologies, *e.g.*, the $O(10^3)$–$O(10^5)$ species used in metallurgy, polymer technologies, biotech, and the pharmaceutical industry. The currently used "high tech" semiconductors also provide but a limited set of relevant materials properties, such as band gaps, lattice constants, effective masses and mobilities. Of course, there are good historical reasons for this narrowness of material base, ranging from the stringent criteria which electronic devices place on material perfection and purity, to the natural human inertia associated with the large investments that have been made in the first semiconductor to work in a big way. Given, however, the remarkable progress in our ability to grow high-purity artificial structures, (even in defiance of conventional equilibrium thermodynamics), and the increasing need to diversify materials properties in new device architectures, one wonders whether time has come to take another, systematic look at enlarging the data base of potentially useful electronic materials and structures. The obvious approach to this need is to use educated, phenomenological trial-and-error techniques that have brought us, among others, new superconductors, ferroelectrics, and quasicrystals. It is almost certaln that a combination of such Edisonian approaches with a considerable amount of "guided luck" will continue to provide us with exciting new materials. There is, however, a possible complementary approach: use of solid state theory as a guide to selecting promising new materials. This article outlines a possible methodology for systematic predictions of stable materials and their properties.

2. General Strategies for Predicting New Compounds

One approach for searching for new compounds is to limit oneself to a *known class* of materials with a known crystal structure, and to search for *new members* in this class. Examples include the 1984 prediction by Jaffe and Zunger[1] of 22 yet unmade I–III–VI_2 or II–IV–V_2 chalcopyrites (*e.g.*, $ZnSiSb_2$, $CdGeSb_2$, $MgGeP_2$, $MgGeAs_2$, $CuTlTe_2$, $BeCN_2$), or the predicted properties of the I–II–V filled tetrahedral semiconductors[2,3] (*e.g.*, LiZnN, LiZnP, CuMgP, CuZnAs) and their initial experimental testing.[4]

A more general (although less certain) approach is *not* to limit ourselves to a known structure. Instead, one can ask "What are the stable crystal structures that can be made from certain atoms on given substitutional lattices." Indeed, many important solid-state structures can be described as substitutional A/B systems, in which the sites of a crystal lattice are occupied by A and B atoms in different patterns ("configurations"). These include abrupt and intermixed superlattices, substitutional impurities, impurity aggregates, ordered A_pB_q superlattices, and random $A_{1-x}B_x$ alloys. In theoretical studies of the energetics of substitutional systems one requires in principle, sampling of the 2^N possible configurations for placing A and B atoms on N lattice sites. Even limiting N to ~40 sites, this is a formidable task for first-principles electronic structure methods,[5] as it involves an astronomical number of calculations (of the order of the number of stars in this galaxy). Of these configurations, only ~1–5 are stable ground states. In conventional first-principles total energy approaches[5] to a material AB one usually performs the total energy calculation for a 5–10 (rather than 2^N) assumed crystal structures that by analogy with related compounds or by "chemical intuition" are expected to be likely competitors for the stable ground state of AB. Comparison of total energy vs volume curves for such a set of "intuitive structures" permits the identification of the stablest structure in this set. While generally successful, the predictive value of this approach of "rounding up the usual suspects" does depend on one's ability to guess at the outset a set of structures which includes the "winning" (minimum energy) configuration. One wonders, however, if a different, hitherto unsuspected structure could have yet lower energy, or whether a linear combination of two other structures could have a lower energy.

I will discuss here the prospects of the recently developed "cluster expansion methods"[6] which allow one to (i) perform a systematic ground state search among $\sim 10^5$ atomic configurations and, (ii) obtain the temperature-composition phase diagram in a *first-principles manner*, using directly calculated total energies of only $\sim$10–20 configurations. Once a handful of ground state stable structures have been identified, one can proceed and calculate their band structures and other interesting materials properties.

3. Basic Principles of the Cluster Expansion

A general approach to the energetics of substitutional systems is the Cluster Expansion (CE),[6-9] in which the energies of the different configurations are described by a generalized Ising Hamiltonian.[7] In the cluster expansion, the alloy is treated as a lattice problem: One uses a given underlying lattice (fcc, bcc, etc.) and defines a configuration σ by specifying the occupation of each of the N lattice sites by an A atom or a B atom. For each configuration, one assigns a set of fictitious "spin" variables $\hat{S}_i$ ($i=1, 2, \cdots, N$) to each of the N sites of the lattice, with $\hat{S}_i=-1$ if site i is occupied by an A atom, and $\hat{S}_i=+1$ if it is occupied by a B atom. The set of spin variables $\{\hat{S}_i\}$ defines the configuration, σ. One can imagine that the total electronic + nuclear energy of a given configuration σ can be calculated directly from quantum mechanics (using *e.g.*, the local density or the Hartree Fock methods) yielding

$$E_{\text{direct}}(\sigma)=\langle \Psi | H | \Psi \rangle / \langle \Psi / \Psi \rangle. \quad (1)$$

In principle, this can be repeated for each σ. The cluster expansion consists of mapping the set $\{E_{\text{direct}}(\sigma)\}$ onto an Ising-like series:

$$E_{\text{CE}}(\sigma)=J_0+\sum_i J_i\hat{S}_i(\sigma)+\sum_{j<i} J_{ij}\hat{S}_i(\sigma)\hat{S}_j(\sigma) + \sum_{k<j<i} J_{ijk}\hat{S}_i(\sigma)\hat{S}_j(\sigma)\hat{S}_k(\sigma)+\cdots, \quad (2)$$

for configuration σ, where the J's are "interaction energies", and the first summation is over all sites in the lattice, the second over all pairs of sites, the third over all triplets, and so on. These constitute the basic "figures" of the lattice. We have 2^N configurations and 2^N interaction energies, so $E_{\text{direct}}(\sigma)=E_{\text{CE}}(\sigma)$ can be solved. The whole point of the cluster expansion[6] is to find a scheme for obtaining a rapidly convergent series that requires only a small number of calculations. When the final J's are known, the energy $E_{\text{CE}}(\sigma)$ of *any* of the 2^N configurations can be calculated almost immediately. Furthermore, one can readily (i) apply linear programming techniques to find ground state structures,[10] (ii) use statistical mechanics techniques such as the Cluster Variation Method[11a] or Monte Carlo[11b] to calculate phase diagrams, and (iii) calculate the energy of an arbitrarily complex configuration.[12]

The main challenge is then to establish a first-principles theory for obtaining the interaction energies $\{J\}$. There are three general approaches to this problem.

The first approach is to do a purely empirical fit of the J's to known features of the phase diagram for the alloy system.[13] For example, information about the values of the J's may be extracted from experimental critical temperatures.[13] This approach is the simplest, but it provides little new information about the properties of the alloy.

The second approach is to determine the J's by treating ordered structures as perturbations of the random alloy. The random alloy is treated using either the Coherent Potential Approximation (CPA). Methods based on these approaches include the Generalized Perturbation Method (GPM) of Ducastelle and Gautier,[14] and the Concentration-Wave (CW) method of Gyorffy and Stocks.[15] These CPA-based methods currently neglect[6] both positional fluctuations (atomic relaxations) and charge fluctuations, so they apply only to a narrow set of AB materials having small A vs B size and electronegativity difference.

The third approach is the direct inversion method[6,8,9,12,16-23] which was recentiy reviewed.[6] This method is based on the recognition that when the CE converges rapidly, the energies of the 2^N configurations are approximately linearly dependent. In this case, knowing a few of the energies allows us to determine the rest. The method thus extracts the J's from total energy calculations on a set of ordered structures. We first compute $E(\sigma)$ of eq. (1) for a few (10–20) ordered structures (σ) using *ab initio* methods, and then substitute the results on the left hand side of eq. (2). We then solve eq. (2), finding a set $\{J\}$ of interaction energies. These are tested as to their ability to predict the energies of *other* configurations. The method includes in a natural way atomic relaxation as well as charge fluctuation effects. Convergence with respect to the range of the interaction energies is systematically tested. Thus, the advantage of the cluster expansion is that it extracts information from a small set of structures to make predictions for the energies of all other structures; by contrast, direct electronic structure calculations[5] treat each configuration independentiy, and fail to take advantage of the underlying relations among different substitutional configurations of the system.

4. Applications to New Transition Metal Compounds

4.1 *Old and new Pt compounds*

One of the well-known metallurgical rules is that binary transition metal systems whose constituent atoms have nearly-filled d shells ("late transition metals") have *positive* mixing enthalpies ΔH_f and show, at low temperatures, phase-separation rather than long-range ordering. I was wondering if this is valid. Consider for example, the phase-behavior of binary alloys of Pt with its neighboring elements in the Periodic Table.[24,25] First, Pt–Ni and Pt–Cu actually order. Second, while Pt–Rh and Pt–Pd were surmised[24,25] to phase separate, examination of the original data[26] shows no evidence to this effect. In fact, measurements on Pt–Pd have shown *negative* mixing enthalpies[27] and clear evidence in X-ray diffuse scattering[28] for a substantial degree of short-range order which remains unexplained.

We have applied the CE to this problem,[20] using the local density approximation (LDA[5]) within the linear augmented plane wave (LAPW) method.[29] We have used the calculated effective interaction energies $\{J\}$ to perform a

ground state search comparing different structures at the same composition as well as the stability of the homogeneous structure against mixing of two (ordered or disordered) phases of different compositions. The resulting ground state lines are shown in Fig. 1. These show that (i) Pd–Rh phase separates, as found experimentally,[26] but (ii) Pt–Cu, Pt–Pd, and Pt–Rh are predicted to order in [1/2, 1/2, 1/2], [001], and [10 1/2] ordering vectors, respectively. For $Pt_{0.5}Cu_{0.5}$ we correctly find trigonal $L1_1$ ordering showing that our expansion captures the delicate competition between trigonal ($L1_1$) and tetragonal ($L1_0$) structures. No low temperature data exist for Pt–Rh so our result constitutes a prediction for an ordered structure. For $Pt_{0.51}Pd_{0.49}$, X-ray diffuse scattering experiments[28] revealed significant short range order in the nominally disordered alloy; while the crystal structure (or phase diagram) was not determined, the average number of Pt first-neighbors to Pd is consistent with tendencies to order in the structure predicted here. It is interesting to note that our ground-state search (Fig. 1) identifies new structures that were *not used* to determine the interaction energies, *e.g.*, D1 and D7 for Cu–Pt, and $D1_a$ and X2 for Rh–Pt. Hence, the cluster expansion method permits predictions of *unsuspected* ordered structures. These results await experimental testing.

4.2 *Old and new Cu and Ni compounds*

The intermetallic systems Cu–Au, Cu–Pd, Cu–Pt, and Cu–Rh form an interesting set in that while in elemental form, Cu, Pd, Pt, and Rh are all fcc metals, their 50%–50% equimolar compounds exhibit at low temperatures a range of structural symmetries:[24,25] CuAu has the fcc-based ($L1_0$) structure, CuPd has a bcc-based (B2) structure, CuPt has a rhombohedral ($L1_1$) structure, and CuRh does not exist (it phase separates into pure Cu+Rh). We have applied the CE method to these systems[19] in a parallel way to what was described earlier for the Pt systems. For Cu–Pd and for Ni–Al we also do a parallel CE for fcc vs bcc structures.

Figure 2 depicts the ground-state lines for the Cu-based alloy systems studied here and for Ni–Al. The sym-

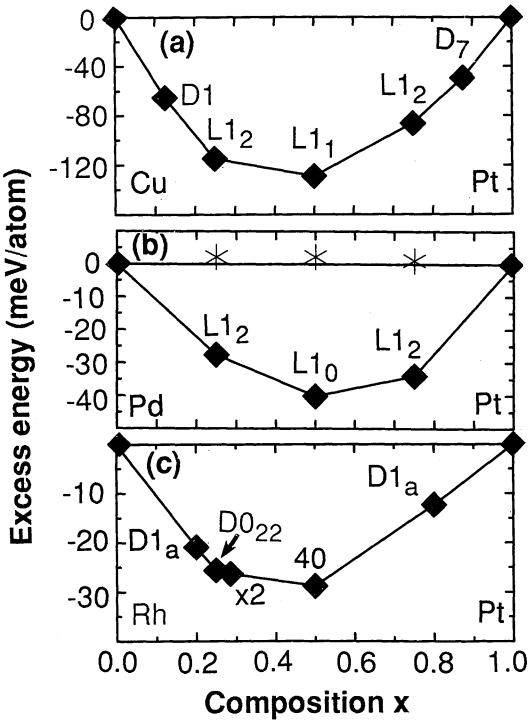

Fig. 1. Predicted $T=0$ ground states (diamond-like symbols) of Pt-based binaries as a function of composition. $D1_a$ is the $MoNi_4$-type A_4B superlattice along [201]. "X_2" is the A_5B_2 superlattice along [201] and D1 (A_7B) and D7 (AB_7) are fcc-like structures with the unit cell vectors double that of the underlying fcc unit vectors. Crosses in part (b) show non-relativistic results that indicate that in the absence of relativistic effects the ground state of Pt–Pd is phase separating. From ref. 20.

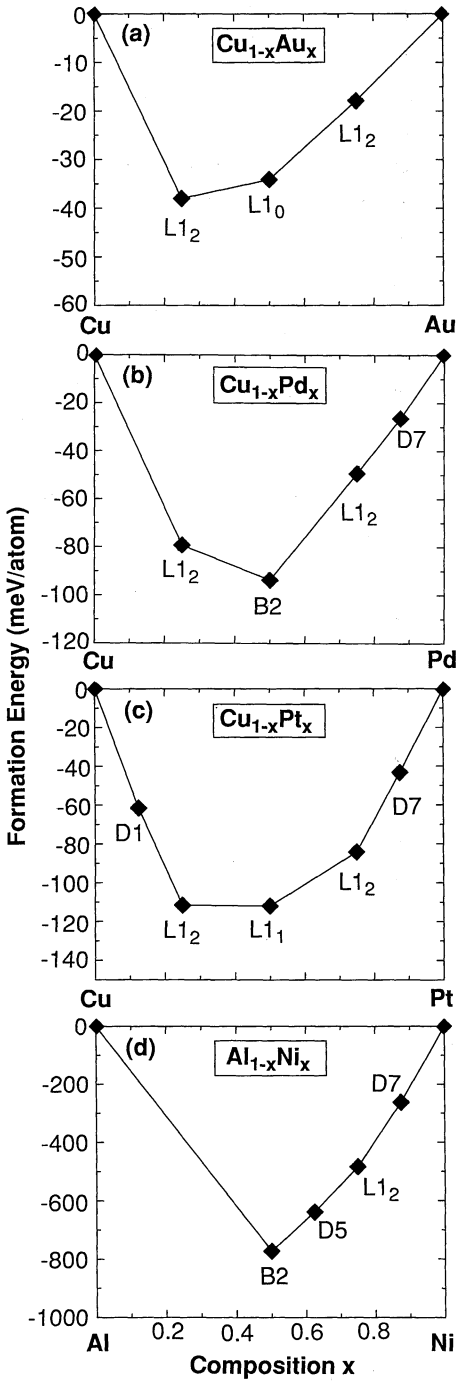

Fig. 2. Predicted $T=0$ ground-state line for (a) $Cu_{1-x}Au_x$, (b) $Cu_{1-x}Pd_x$, (c) $Cu_{1-x}Pt_x$, (d) $Cu_{1-x}Rh_x$ and (e) $Al_{1-x}Ni_x$. From ref. 19.

metries established clearly from experiment[24] are also found theoretically, even though we have purposely omitted from the basis set used to extract J_F some of the structures which are *known* to be ground states. Note the new compound ("D7") predicted for Ni_7Al.

We next tested whether this new ground state structure is stable at finite temperatures. This requires calculating the *free* energies of eq. (2) using the cluster variation[11a] or Monte-Carlo[11b] methods. Here we used the former. Figure 3(a) gives the observed[24] Ni-Al phase diagram; the calculated fcc and bcc solid phase portions of the $Al_{1-x}Ni_x$ phases diagram are given in Fig. 3(b). The new "D7" structure Ni_7Al is predicted to be stable up to ≈ 900 K. This phase has never been reported, but the observed instability of the binodal might be indicating the presence of a hidden phase like our D7. Since this phase has a very low Al concentration, and since its translation vectors are fcc-like (but doubled), this phase might be easily confused with fcc Ni with a random distribution of Al impurities. It awaits experimental testing.

5. New, Surface-Stabilized Ternary Semiconductors

A generally interesting question is whether one can make *surface-stabilized* ordered structures that have no counterpart in the *bulk* phase diagrams. It is possible to apply the cluster expansion formalism to *surface* thermodynamics by replacing the calculated *bulk* energies of eq. (1) with *surface* formation energies.[30,31] The latter calculations involve both surface relaxation and surface reconstructions. Indeed, it has recently been noted that numerous III-V alloys exhibit in vapor phase growth *spontaneous* long-range ordering in the form of monolayer $(AC)_1/(BC)_1$ superlattices in the (111) orientation[32] (the "CuPt-like structure"). The degree of ordering is never perfect; it can however, be maximized in certain growth temperature ranges and substrate misorientations. An extended list of observations of CuPt ordering is given in ref. 32. In all cases, ordering occurred as a result of *homogeneous* alloy growth *without* sequential (shutter-controlled) exposures. *Bulk* phase diagrams of $Ga_xIn_{1-x}P$ show no ordering. To see whether such novel ordered structures can be explained by surface stabilization, we have applied our *surface* CE of eqs. (1) and (2) to the $Ga_{0.5}In_{0.5}P/GaAs(001)$ surface. Total energy calculations showed that the CuPt-surface contains homopolar Ga-Ga and In-In dimers, whereas the chalcopyrite surface exhibits heteropolar dimers.[30] We find that surface reconstructions (dimerization, buckling, and tilting) considerably lower the $T=0$ energy of all the surfaces and, most significantiy, make the surface corresponding to the CuPt ordering the lowest energy. Thus, surface reconstruction favors atomic arrangements that are unstable in the bulk.

To see if the $T=0$ energy differences between different surface structures are sufficient to preserve any type of order at typical growth temperatures, we calculated[31] the CuPt order parameter η, as a function of temperature using the cluster variation approach[11a] to eq. (2). For the CuPt structure, perfect ordering gives $\eta=1$. Figure 4 displays the results for $\eta(T)$, of the cation-terminated surface. For the *unreconstructed* case, the system undergoes a phase transition to the disordered phase at $T_c=146$ K. It is clear that at growth temperatures (typically 900 K) no traces of long-range $CuPt_B$ ordering are to be expected with an unreconstructed surface. For the *reconstructed case*, on the other hand, the CuPt order parameter η is seen to be significant at growth temperatures (*e.g.*, $\eta \approx 0.87$ at $T=900$ K). Thus, surface effects stabilize the bulk-unstable CuPt ternary compound even at growth temperatures. Reference 32 discusses a few scenarios of this surface-stable structure growth.

6. Electronic Properties of CuPt-Like Ternary Semiconductors

This unique phenomenon of spontaneous ordering was

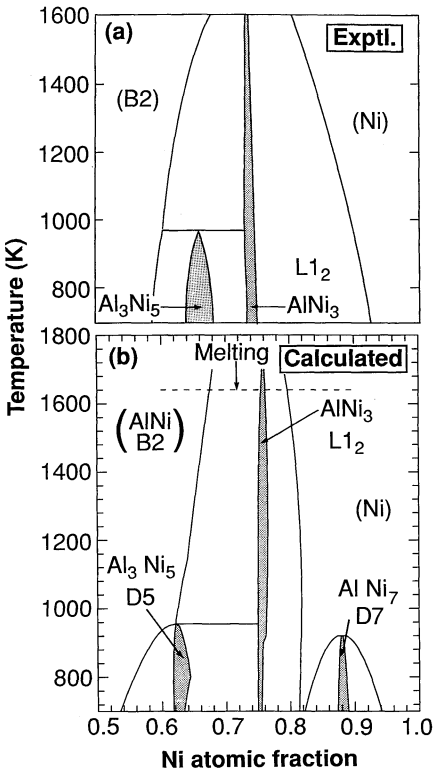

Fig. 3. (a) Experimental[25] and (b) calculated[19] phase diagram of Ni-rich $Al_{1-x}Ni_x$. Note the predicted new Ni_7Al phase.

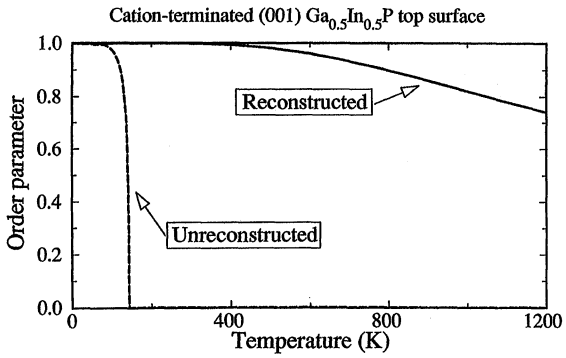

Fig. 4. Calculated CuPt long range order parameter η for the cation-terminated $Ga_{0.5}In_{0.5}P$ (001) surface. Note how reconstruction eliminates the low-temperature critical transition, replacing it by a continuous transition in which sigriificant ordering exists even at growth temperature (~ 900 K). From ref. 31.

predicted to alter the alloy's band structure in a significant way.[33,34] The basic mechanism can be appreciated as follows. Denoting superiattice (SL) states by an overbar and the homogeneous alloy states by angular brackets, folding relations show that in a monolayer $(AC)_1(BC)_1$ (111) superlattice the states at the $\bar{\Gamma}$ point are constructed from the zincblende-like states at $\langle\Gamma\rangle + \langle L^{111}\rangle$. The folded zincblende states at this wave vector are coupled by the perrurbing superlattice potential $\delta V(\underline{r})$. This coupling leads to a "level repulsion" between states of the same symmetry,[33] i.e., the superlattice states are displaced relative to the unperturbed states. For example, the $\bar{\Gamma}$-folding alloy states $\langle\Gamma_{1c}\rangle$ and $\langle L_{1c}\rangle$ couple through δV, producing the superlattice states $\bar{\Gamma}_{1c}^{(1)}$ and $\bar{\Gamma}_{1c}^{(2)}$ that are lowered and raised, respectively, relative to the averaged alloy states. The downward displacement of the $\bar{\Gamma}_{1c}^{(1)}$ (the conduction band minimum, or CBM) and the upward displacement of the $\bar{\Gamma}_{3v}^{(2)}$ (the valence band maximum, or VBM) reduce the band gap. Theoretical details describing this mechanism are given in refs. 33 and 34. Figure 5 shows predictions for band gap reductions through spontaneous ordering for many systems. It illustrates how the direct band gap of the random alloy at $x=1/2$ changes if the alloy orders in the monolayer (201) structure ("chalcopyrite"), the (001) structure ("CuAu"), or the (111) structure ("CuPt"). These results pertain to perfect ordering, i.e., $\eta=1$. It was pointed out (see review in ref. 32) that the band gap

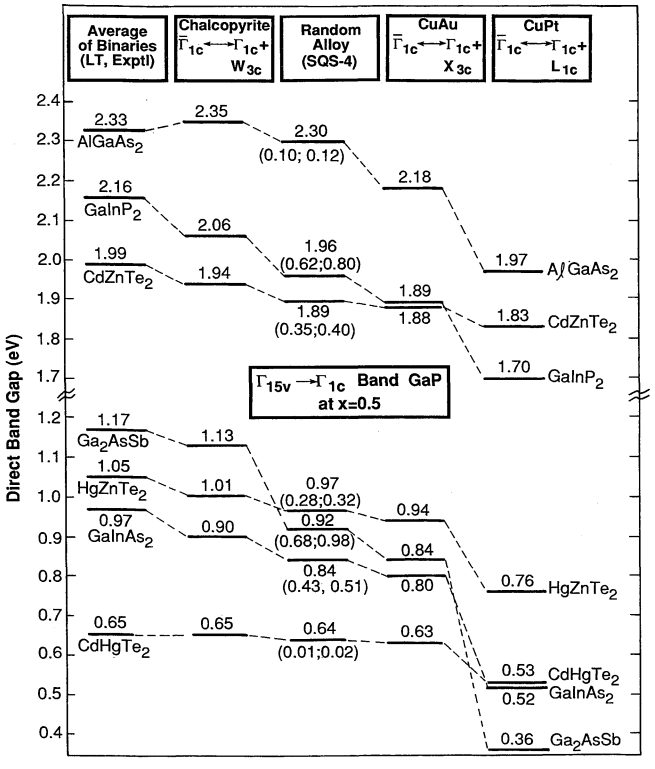

Fig. 5. Calculated direct band gaps of various 50%–50% ordered alloys of III–V and II–VI systems. The band gaps of the random alloy are cited here with respect to the crystal-field averaged VBM. To obtain the value with respect to the VBM (using $GaInP_2$ as an illustration) we calculate $1.96+(0.80-0.62)/4=2.01$ eV. Hence, the band-gap reduction in the CuPt structure relative to the VBM of the random alloy is $1.70-2.01=-0.31$ eV. From ref. 34.

reduction depends (quadratically) on the *degree* η of long range ordering. Hence, a variable gap over a significant spectral range can be obtained by controlling the degree of ordering.

This mechanism of ordering-induced band gap reduction can lead to the interesting opportunity of tuning alloy band gaps *at a fixed composition*, by selecting those growth conditions that induce spontaneous ordering. Reference 34 lists may common semiconductor alloys and gives their predicted band gaps for a few forms of crystallographic order. Such effects have also been seen experimentally[35] in $GaInP_2$. This mechanism of ordering-induced band gap narrowing has been recentiy proposed[36] to yield $\sim 10\mu$ band gap in spontaneously-ordered $Ga_{1-x}In_xSb$ and $InAs_{1-x}Sb_x$ alloys. Initial experimental results[37] appear very encouraging. Another example is the prediction of ref. 38 that (111)-oriented AlAs/GaAs superlattice (SL) (the CuPt structure) will have direct band gaps despite the fact that short-period AlAs/GaAs SL's oriented along (001) are known to have an indirect band gap. Recent experimental resuits[39] have failed, however, to find a direct gap in (111)-oriented AlAs/GaAs SL's. The authors[38] believe, however, that these (111) samples may not exhibit sufficiently abrupt interfaces to reveal the properties of true (111) SL's. To test this, Laks and Zunger[40] have recently formulated theoretical approaches that predict the value of the band gap as a function of the interfacial roughness. It was shown, for example[40] that while in an *abrupt* (001)-oriented monolayer GaAs/AlAs superiattice the lowest gap (1.93 eV) is an L-derived GaAs-like state, in a *locally interdiffused* SL the gap reverts to the 2.08 eV X^{xy}-derived AlAs state. This suggests the possible use of the degree of interfacial abruptness as a new degree of freedom in tuning band gaps.

All previous examples pertain to use of ordering without strain to get new band gaps. Biaxial strain can, however, be used to reduce band gaps.[41] The basic idea here is to take a material with a small band gap and small lattice constant (SGSL) and layer it coherently with a material having a larger gap and larger lattice constant (LGLL), forming a strained-layer $(SGSL)_p/(LGLL)_q$ superlattice. Coherence of SGSL with LGLL then *expands* the lattice constant of SGSL parallel to the interface, thus lowering its Γ conduction-band minimum. At the same time, tetragonal *compression* of SGSL in the perpendicular direction splits its valence band maximum, raising the energy of the upper split components. Both effects act to reduce the band gap relative to unstrained bulk SGSL. This approach has been proposed by Osbourn[41] for $SGSL=InAs_{0.39}Sb_{0.62}$ and $LGLL=InAs_{1-x}Sb_x$ with $x>0.61$. Since quantum confinement effects at small (p, q) act in the opposite direction (increasing the band gap) relatively thick layers are needed to achieve the maximum band-gap narrowing.[41] Yet, the need to accommodate coherently the misfit strain limits the maximum thickness that can be used.

Biaxial strain has also been used recently to make a few predictions, *e.g.*, (i) use of strain to convert the *normally-indirect* $(GaAs)_1(GaP)_1$ SL grown on a lattice matched substrate into a direct gap superlattice $(GaAs)_1(GaP)_1$

grown on GaAs[42] (rather than the alloy). There are now experimental confirmations of this idea.[43] (ii) Use of strain to convert the *indirect* gap Si_nGe_n SL grown on Si to a *direct* gap SL when grown on $Si_{0.5}Ge_{0.5}$ or on pure Ge substrates.[44] The experimental results here are yet inconclusive; there are, however, strong ongoing interactions between experimentalists and theorists to clarify this situation.[45] Again, the research opportunities here are almost unlimited, once one realizes the basic design principle of use of biaxial strain.

7. Chalcopyrite-Zincblende Alloys and Compounds

Many interesting alloys exhibit competition of *three* atomic species on the same lattice. Semiconductor examples include the technologically-important (in solar cells) $(CuInSe_2)_x(ZnSe)_{2x}$ system in which Cu, In, and Zn can reside on the fcc lattice. More generally, we have an alloy of $A_{1-x}B_xC$ with DC. We will address here the $x=1/2$ problem. The statistical mechanis[46] was addressed in two steps. First, we consider the occupations of the fcc cation sublattice by A and B atoms in the $A^{I}_{0.5}B^{III}_{0.5}C^{VI}$ chalcopyrite system. Second, we add the third cation D^{II} competing for the same sublattice. In addressing the first problem we consider the spin-1/2 Ising model where site i is occupied by either an A atom ($\sigma_i=-1$) or by a B atom ($\sigma_i=+1$). This pertains to $CuInSe_2$ with Cu=A and In=B. We take the Ising Hamiltonian for an arbitrary configuration σ of this binary system to be

$$H_{\text{bin}}(\sigma)=\tilde{J}_0\sum_{(ij)}J_{ij}\sigma_i\sigma_j+\sum_{(ijkl)}J_{ijkl}\sigma_i\sigma_j\sigma_k\sigma_l, \qquad (3)$$

where (ij) indicates a summation over all pairs, and $(ijkl)$ indicates a summation over all tetrahedra in the lattice. To find the values of the interaction parameters $\{J\}$ we fit eq. (3) to a set of directly calculated LDA formation enthalpies $\Delta H(\sigma)$ of simple CuSe/InSe ordered structures at the equilibrium volume. Retaining only $\tilde{J}_0$, J_2, and J_4 in the Hamiltonian of eq. (3) gives a very good fit. The order-disorder transition obtained in a Monte-Carlo (MC) simulation for $CuInSe_2$ is[46] $T_c=1120$ K, in perfect agreement with the result using up to fourth-neighbor pair interacllons (the experimental result is 1083 K). The CVM tetrahedron approximation leads to $T_c=1224$ K.

The consideration of the pseudoternary case $(ABC_2)_{1-x}$-$(DC)_{2x}$ (*e.g.*, $CuInSe_2$-ZnSe) requires two changes. First, a generalization to a spin-1 Hamiltonian, representing occupations of site i by A ($S_i=1$), B ($S_i=1$), and D ($S_i=0$) is needed. Second, the added interaction terms are now *volume-dependent* since the end-point chalcopyrite and zincblende constituents can have different equilibrium molar volumes, in contrast to the pseudobinary case, where all structures $(CuSe)_p(InSe)_p$ had the same composition and, hence, nearly equal molar volumes. We will therefore use a nearest-neighbor spin-1 Ising model (a generalized Blume-Emergy-Griffiths,[47] or BEG model) with volume-dependent interactions:

$$H_{\text{tern}}(S,V)=[J_2\sum_{\langle ij\rangle}S_iS_j+J_4\sum_{\langle ijkl\rangle}S_iS_jS_kS_l]+J_0(V)+D(V)\sum_i S_i^2-K(V)\sum_{\langle ij\rangle}S_i^2S_j^2. \qquad (4)$$

The terms in brackets are the nearest-neighbor terms of eq. (3). All odd terms were omitted, assuming that the Hamiltonian is invariant under the A↔B interchange.

Using the LAPW method we have calculated the volume-dependent total energies E_S for structures S=ZB, CH, and stannite ST, finding also the equilibrium volumes V_S. We solved the statistical mechanics of eq. (4) in the CVM tetrahedron approximation.[11a] Figure 6 shows the calculated phase diagrarns of $(CuInSe_2)_{1-x}$-$(ZnSe)_{2x}$, using a hierarchy of approximations in the Hamiltonian of eq. (4). The diagram of case (i) corresponds to the antiferromagnetic spin-1 Ising model in the fcc sublattice. The diagram of case (ii) shows the role of positive K values: it widens the CH-ZB miscibility gaps, suppressing the small second-order transition line present in case (i) between ≈410 and 550 K, and removes the triple point. The diagram of case (iii) shows that J_4 acts to reduce considerably the transition temperatures in the low-x region and to reduce the width of the CH-ZB miscibility gap. Finally, the use of volume-dependent interactions acts to increase the CH-ZB miscibility gap

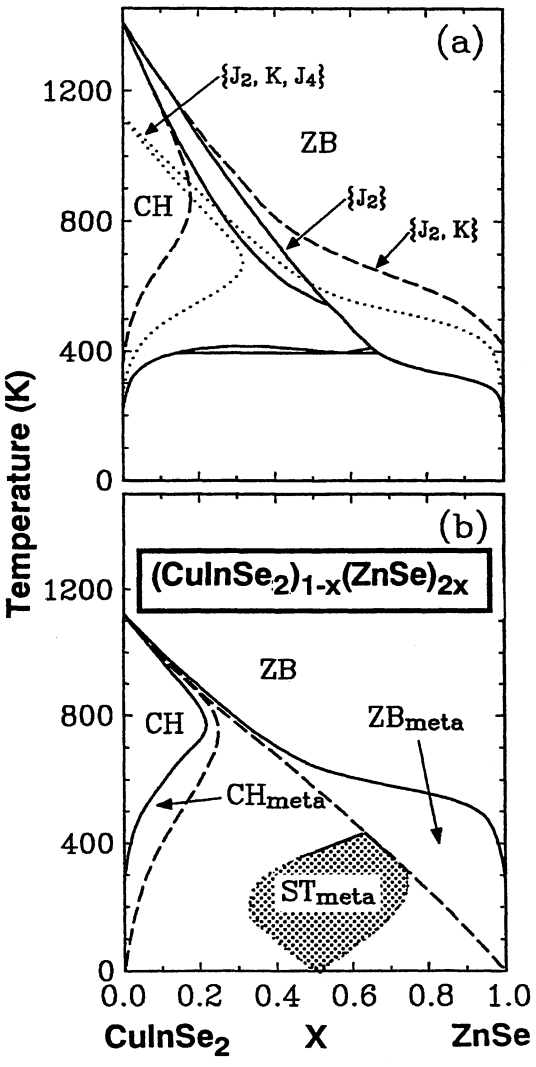

Fig. 6. Calculated phase diagram of $CuInSe_2$/ZnSe using a few representations: (a) J_2-only; J_2+K_2; $J_2+K_2+J_4$. In (b) we show the result including volume-dependent interaction energies. From ref. 46.

[Fig. 6(b)]. The maximum equilibrium solubility of ZnSe in $CuInSe_2$ with the chalcopyrite structure is 22% (at $T \approx 770$ K), while $CuInSe_2$ becomes completely soluble in ZnSe with the zinc-blendestructure above the order-disorder temperature of $CuInSe_2$. Our results hence show that, contrary to the other known heterostructural ternary alloy $(GaAs)_{1-x}Ge_{2x}$, characterized by vanishing solid solubility, $(CuInSe_2)_{1-x}(ZnSe)_{2x}$ should exhibit substantial miscibility. Additional metastable features are presented for this *ab initio* phase diagram. The left dashed line in Fig. 6(b) marks the chalcopyrite spinodal, which is the upper-composition limit of metastability for the CH phase. The right dashed line is the unstable second-order transition line inside the coexistence region and marks the lower-composition limit for metastability of the zinc-blende phase. Between these two lines we find $\partial^2 F/\partial x^2 < 0$, which implies that any incipient phase separation will be preferred to a single-phase state. Since at $x = 1/2$ we found $0 < \Delta H(ST) < \Delta E_{VD} < \Delta E_{Rand}$, the stannite structure could be observed in $(CuInSe_2)_{1-x}(ZnSe)_{2x}$ if *long-range* atomic diffusion were inhibited. The shaded region at $x \sim 1/2$, $T < 440$ K shows this marginally *metastable ST* phase. It should be observed if *short-range* atomic rearrangements are allowed but *long-range* atomic migration (and hence, phase separation) is slow at $T < 440$ K. The chalcopyrite-forbidden X-ray diffraction peaks at (001), (110), (112), and (221) $2\pi/a$ characterize the ST phase. It would be very interesting to measure such X-ray reflections in chalcopyrite-zincblende alloys to see if the stannite structure is stabilized. Recently, Gallardo[48] suggested that such a phase could exist in solid solutions of $AgInSe_2$ with HgSe. To test this, Lu and Zunger[49] calculated (using the LAPW method) the formation enthalpy of the relevant Stannie phases. While for $CuInSe_2/2SnSe$, Osorio *et al.*[46] found $\Delta H_f = +25.6$ meV/4-atoms, Lu and Zunger found[49] for $AgInSe_2/2HgSe$ a much smaller number of 2.6 meV/4 atoms. Thus, this stannite phase could be stable!

8. Epitaxial Stabilization of New Semiconductors

Section 5 showed how surface reconstruction can stabilize a structure that is bulk unstable. Another effect is the use of epilaxial strain to stabilize thermodynamically a bulk-unstable compound.[50,51] Figure 7 gives a calculated example:[51] MgS is stable in the NaCl (B1) structure, so the total energy vs lattice constant curve has a minimum for that structure, whereas the zincblende (B3) phase is higher in energy. To stabilize zincblende MgS, one can grow it epitaxially on a substrate whose lattice constant is larger than a_s^*. Then, the epitaxial (dashed line) B3 energy is lower than the epitaxial B1 energy. References 50 and 51 discuss in detail how such predictions are made, what is the film thickness for which epitaxial stability is maintained, and how one can make zincblende NaCl or NaCl-type CdTe.

9. Summary

We have shown how total energy LDA calculations of O(10) ordered structures can be used to extract the "building blocks" interaction energies $\{J_F\}$, and how these can be used in conjunction with lattice statistical mechanics techniques to calculate thermodynaniic properties. The quantities that can be calculated in this way include: (i) identification of the $T=0$ lowest energy configuration out of 2^N possibilities, (ii) formation energies of "complex" structures, not amenable to *direct* LDA calculations, (iii) excess configurational enthalpies, entropies, and free energies as a function of (x, T), (iv) composition-temperature phase diagrams, (v) SRO and LRO parameters as a function of (x, T), and (vi) equilibrium lattice constants, interatomic distances, and elastic constants as a function of (x, T).

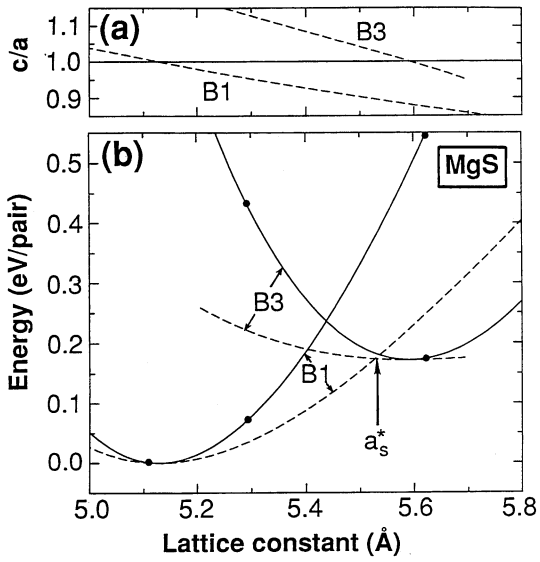

Fig. 7. Calculated bulk (solid line) and epitaxial (dashed lines) total energies of MgS in the zincblende (B3) and NaCl (B1) structures. The top figure shows the c/a ratio. From ref. 51.

The systems for which the method has been illustrated include (a) pseudobinary $A_{1-x}B_xC$ semiconductor alloys, (b) binary $A_{1-x}B_x$ transition metal alloys, (c) Ternary alloys such as $CuInSe_2/ZnSe$, (d) epitaxial phase diagrams, and (e) surface phase diagrams. The main advantages of this method lie in its ability to predict unsuspected structures and to *analyze* trends in the above quantities in terms of electronic structure constracts, thus helping to demistify the highly successful Pauling-esque rules of metallurgy and structural solid-state chemistry.

The main predictions discussed here are: (i) new chalcopyrites and pnictides (see ref. 1); (ii) I–II–V filled tetrahedral compounds (refs. 2–4); (iii) new ordered phases for Pt–Pd and Pt–Rh (ref. 20); (iv) a new Ni–Al structure (ref. 19); (v) ternaiy III–IV–V_2 CuPt-like semiconductors (ref. 32) having new gaps (ref. 34); (vi) direct-gap AIAs/GaAs (111) superlattices (ref. 38); (vii) direct gap GaAs/GaP superlattices grown on GaAs (ref. 42); (viii) stannite ordering in $CuInSe_2/ZnSe$ (ref. 46) and $AgInSe_2/HgSe$ (ref. 49); (ix) epitaxial stabilization of the NaCl structure of CdTe or the zincblende structure of NaCl (ref. 50).

This work was supported by DOE (Office of Energy Research and Office of Conservation and Renewable) through grant DE-AC02-83-CH10093.

References

1) J. E. Jaffe and A. Zunger: Phys. Rev. B **29** (1984) 1882.

2) D. M. Wood and A. Zunger: Phys. Rev B **34** (1986) 4105.
3) A. E. Carlson, D. M. Wood and A. Zunger: Phys. Rev. B **32** (1985) 1386; S. H. Wei and A. Zunger: Phys. Rev. Lett. **56** (1986) 528; D. M. Wood, A. Zunger and R. de Groot: Phys. Rev. B **31** (1985) 2570; N. E. Christensen: Phys. Rev. B **32** (1985) 6490.
4) K. Kuriyama and F. Nakamura: Phys. Rev. B **36** (1987) 4439 and Appl. Phys. Lett. **69** (1991) 7812; R. Bacewicz and T. F. Ciszek: Appl. Phys. Lett. **52** (1988) 1150; A. Nelson, M. Engelhardt and M. Hochst: J. Elect. Spect. **51** (1990) 623.
5) Recent books summarizing modem electronic structure methods include *Electronic, Structure, Dynamics, and Quantum Structural Properties of Condensed Matter*, eds. J. T. Devereese and D. Van-Camp (Plenum, New York, 1985).
6) For a review of the cluster expansion method see A. Zunger: *NATO Advanced Study on "Statics and Dynamics of Alloy Phase Transformations"* (Plenum Press, 1993).
7) D. de Fontaine: *Solid State Physics*, eds. H. Ehrenreich, F. Seitz and D. Turnbull (Academic, New York, 1979) Vol. 34, p. 73.
8) J. W. D. Connolly and A. R. Williams: Phys. Rev. B **27** (1983) 5169.
9) L. G. Ferreira, S.-H. Wei and A. Zunger: Phys. Rev. B **40** (1989) 3197; S.-H. Wei, L. Ferreira and A. Zunger: Phys. Rev. B **41** (1990) 8240; R. G. Dandrea, J. E. Bernard, S.-H. Wei and A. Zunger: Phys. Rev. Lett. **64** (1990) 36; A. A. Mbaye, L. G. Ferreira and A. Zunger: Phys. Rev. Lett. **58** (1987) 49; S.-H. Wei, L. G. Ferreira and A. Zunger: Phys. Rev. B **45** (1992) 2533; L. G. Ferreira, A. A. Mbaye and A. Zunger: Phys. Rev. B **37** (1988) 10547.
10) J. Kanamori and Y. Kakehashi: J. Phys. (Paris) **38** (1977) 274; F. Ducastelle: *Order and Phase Stability in Alloys* (North Holland, Amsterdam, 1991).
11) (a) R. Kikuchi: J. Chem. Phys. **60** (1974) 1071; Phys. Rev. **81** (1951) 988; (b) N. Metropolis, A. W. Rosenbluth, M. V. Rosenbluth, A. Teller and E. Teller: J. Chem. Phys. **60** (1974) 1071.
12) R. Magri, J. E. Bernard and A. Zunger: Phys. Rev. B **43** (1991) 1593.
13) R. Kikuchi, J. M. Sanchez, D. de Fontaine and H. Yamaguchi: Acta Metall. **28** (1980) 651; J. M. Sanchez, J. R. Barefoot, R. N. Jarrett and J. K. Tien: Acta Metall. **32** (1984) 1519.
14) F. Ducastelle and F. Gautier: J. Phys. F **6** (1976) 2039.
15) B. L. Gyorffy and G. M. Stocks: Phys. Rev. Lett. **50** (1983) 374.
16) K. Terakura, T. Oguchi, T. Mohri and K. Watanabe: Phys. Rev. B **36** (1987) 2169.
17) J. M. Sanchez: Solid State Commun. **65** (1988) 527.
18) A. E. Carlsson: Phys. Rev. B **40** (1989) 912.
19) Z. W. Lu, S.-H. Wei, A. Zunger, S. Frota-Pessoa and L. G. Ferreira: Phys. Rev. B **44** (1991) 512; L. G. Ferreira, S.-H. Wei and A. Zunger: Int. J. Supercomput. Appl. **5** (1991) 34.
20) Z. W. Lu, S.-H. Wei and A. Zunger: Phys. Rev. Lett. **68** (1992) 1961; also Europhys. Lett. **21** (1993) 221.
21) Z. W. Lu, S.-H. Wei and A. Zunger: Phys. Rev. B **45** (1992) 10314; *ibid* **44** (1991) 3387.
22) R. Magri, S.-H. Wei and A. Zunger: Phys. Rev. B **42** (1990) 11388.
23) R. Magri and A. Zunger: Phys. Rev. B **44** (1991) 8672.
24) P. M. Hansen: *Constitution of Binary Alloys* (McGraw-Hill, New York, 1958).
25) T. B. Massalski: *Binary Alloy Phase Diagrams* (American Society for Metals, Metals Park, OH, 1986).
26) E. Raub: J. Less Common Met. **1** (1959) 3.
27) J. B. Darby and K. M. Myles: Metallurg. Transact. **3** (1972) 653.
28) A. Kidron: Phys. Lett **25A** (1967) 112.
29) S.-H. Wei and H. Krakauer: Phys. Rev. Lett. **55** (1985) 1200; also *ibid* **55** (1985) 566.
30) S. Froyen and A. Zunger: Phys. Rev. Lett. **66** (1991) 2132; J. E. Bernard, S. Froyen and A. Zunger: Phys. Rev. B **44** (1991) 11; also *ibid* **44** (1991) 178.
31) R. Osorio, J. E. Bernard, S. Froyen and A. Zunger: Phys. Rev. B **45** (1992) 11, *ibid* **44** (1992) 173, J. Vac. Sci. Technol. B **10** (1992) 1683.
32) For a review of spontaneous ordering in semiconductor alloys see A. Zunger and S. Mahajan in *Handbook of Semiconductors* (Elsevier, Amsterdam, 1993) 2nd ed., Vol. 3.
33) J. Bernard, S. H. Wei, D. M. Wood and A. Zunger: Appl. Phys. Lett. **52** (1987) 311.
34) S.-H. Wei and A. Zunger: Appl. Phys. Lett. **56** (1990) 662.
35) T. Suzuki *et al.*: Jpn. J. Appl. Phys. **27** (1988) 2098; T. Nishino *et al.*: Appl. Phys. Lett. **53** (1988) 583.
36) S.-H. Wei and A. Zunger: Appl. Phys. Lett. **58** (1991) 2684.
37) S. R. Kurtz, L. R. Dawson, R. M. Biefeld, D. M. Follstaedt and B. L. Doyle: Phys. Rev. B **46** (1992) 1909.
38) S. H. Wei and A. Zunger: Appl. Phys. Lett. **53** (1988) 2077.
39) R. Cingolani, L. Tapper and K. Ploog: Appl. Phys. Lett. **56** (1990) 1233.
40) D. B. Laks and A. Zunger: Phys. Rev. B **45** (1992) 11; also *ibid* **45** (1992) 411.
41) G. C. Osboum: J. Vac. Sci. Technol. B **2** (1984) 176.
42) R. G. Dandrea and A. Zunger: Appl. Phys Lett. **57** (1990) 1031.
43) T. Takarohashi and M. Ozeki: Japan. J. Appl. Phys. **30** (1991) L956; J. Cryst. Growth **115** (1991) 538.
44) S. Froyen, D. M. Wood and A. Zunger: Phys. Rev. B **36** (1987) 4547; **37** (1988) 6893; Phys. Rev. Lett. **62** (1989) 975; Appl. Phys. Lett. **54** (1989) 2435; Thin Solid Films **183** (1989) 33.
45) See review on SiGe superlattice by T. P. Pearsall in *Semiconductors and Semimetals* (Academic Press, NY, 1990) Vol. 32, p. 1.
46) R. Osorio, Z. W. Lu, S.-H. Wei and A. Zunger: Phys. Rev. B **47** (1993) 9985; S.-H. Wei, L. G. Ferreira and A. Zunger: Phys. Rev. B **45** (1992) 2533; R. Osorio, S. Froyen and A. Zunger: Solid State Commun. **78** (1991) 249.
47) M. Blume, V. J. Emery and R. B. Griffith: Phys. Rev. A **4** (1971) 1071.
48) P. Grima Gallardo: Phys. Stat. Sol. **134** (1992) 121; *ibid* **119** (1992).
49) Z. W. Lu and A. Zunger: unpublished.
50) For a review of epitaxial stabilization effects see A. Zunger, Handbook of Crystal Growth, Vol. 3, Thin Films and Epitaxy, edited by D. T. J. Hurle (in press).
51) S. Froyen, S.-H. Wei and A. Zunger: Phys. Rev. B **38** (1988) 10124; J. L. Martins and A. Zunger: Phys. Rev. Lett. **56** (1986) 1400.